

Jyoti C. kolte  
Poornima University Jaipur  
[Jyoti180181@gmail.com](mailto:Jyoti180181@gmail.com)

Payal Bansal  
Poornima University Jaipur  
[payal.Bansal@poornima.org](mailto:payal.Bansal@poornima.org)

Ashwini Kumar  
Poornima University Jaipur  
[ashwini.kumar@poornima.org](mailto:ashwini.kumar@poornima.org)



**Abstract**—This paper presents a novel tri-band antenna achieved through Characteristic Mode Analysis (CMA). The antenna's tri-band characteristics are realized by exciting two orthogonal modes and one higher-order mode at 2400 MHz, 3500 MHz, and 5200 MHz for Wi-Fi, 5G Sub-6, and WiMAX applications, respectively, with a broadside radiation pattern. The proposed antenna design involves modifying a circular patch antenna by inserting three equilateral triangle slots. The surface current distribution is reshaped during the antenna modification to achieve the desired frequencies with broadside radiation patterns. The addition of equilateral triangle slots increases the surface current path, resulting in a miniaturized antenna structure with size  $0.32\lambda_o \times 0.32\lambda_o \times 0.01\lambda_o$  in which  $\lambda_o$  is wavelength of lower band 2400MHz. All required modes are stimulated using a  $50\Omega$  coaxial feed line in full-wave electromagnetic simulation after the optimization of the proposed antenna using CMA. The proposed antenna's prototype is made of low-cost FR4 material and is validated by experimentation. The measured operating resonance frequencies, with impedance bandwidths at  $S_{11} \leq -10$  dB, are found to be 2395 MHz (2380-2420MHz), 3500 MHz (3450-3550MHz), and 5283 MHz (5200-5348). Corresponding broadside gains are measured at 5.6 dBi, 6.3 dBi, and 6.9 dBi, respectively. There is good agreement between the simulated and measured results for the proposed antenna. It has a single feed, a low profile, a cost-effective design, and improved gain in addition to stable broadside radiation patterns.

**Index Terms**—Wi-Fi, 5G Sub-6, Wi-Max, Tri-Band Antenna, Characteristic Mode Analysis.

## I. INTRODUCTION

With the proliferation of diverse wireless communication standards, there is a strategic push to integrate as many standards as possible into a single wireless device. This integration includes the 5G Sub-6 band, Wireless Area Network (WLAN), Wi-Fi, and Worldwide Interoperability for Microwave Access (WiMAX) protocols. Researchers worldwide are actively exploring methods to multi band compact antennas, ensuring they remain compact without compromising essential properties for contemporary electronic devices [1-5].

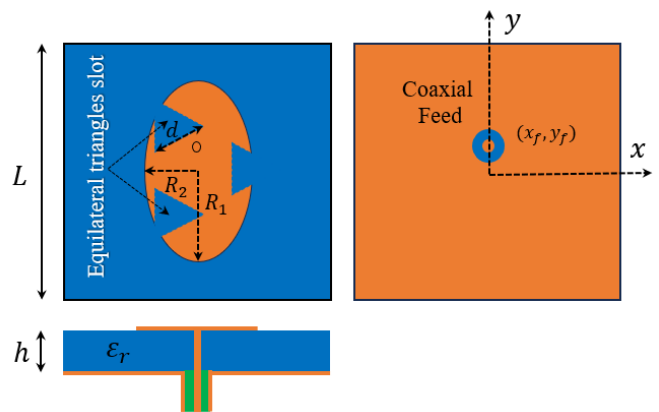


Fig.1. illustrates the tri-band antenna with a coaxial feed as proposed.

Researchers from around the world are actively exploring various methods to design multi-band antennas while maintaining the desired qualities for contemporary gadgets. The need for multifunctional antennas is being driven by a number of applications, including machine-to-machine (M2M) communication, augmented reality, self-driving cars, wireless sensor networks, biomedical implants, and the Internet of Things (IoT). Most of the spectrum that has been set aside for 5G uses by the Federal Frequency Commission (FCC) is in the MM-Wave and Sub-6 GHz bands. By utilizing current base stations, the sub-6 GHz spectrum is intended to be allocated for 5G with the goal of accelerating deployment. This has various advantages, as [3,6-11] outline.

Patch antennas are commonly used in wireless systems because of their ability to be placed versatily over uneven surfaces and their non-planar structure. These antennas have the following qualities: they are simple, lightweight, affordable, flexible, and small [9–11].

In literature, diverse methods are employed to create multi-band antennas. The Defected Ground Structure (DGS) and slot-based patch design are frequently utilized for this purpose [3, 11-16]. The patch also exhibits multi-band capabilities through its loaded resonator slot [5]. Various optimization techniques, including the genetic algorithm, can be employed to create multi-band antennas [17]. The coplanar waveguide (CPW) with slot and fractal methods can also be utilized to design multi-band and miniaturized antennas [1-2, 4, 6,9,18-19]. While these antennas offer numerous advantages, certain performance aspects, such as size, circuit integration complexity, and broadside radiation performance, still require improvement.

To address the aforementioned issues, a novel antenna design has been proposed on an FR4 substrate, aiming for reduced complexity and simplified fabrication while achieving broadside radiation patterns. The tri-band characteristics are attained by introducing three equilateral triangle slots in an elliptically shaped patch, and the design is further optimized using the characteristics mode analysis method. The following sections constitute the planned antenna design work: The specifics of the proposed antenna design are presented in Section

A. Section B: Using the cavity model approach, it presents the preliminary study of antenna design. Sections C to F: Outline the proposed antenna design process utilizing the Characteristics Mode Analysis (CMA) method. Section G: Offers a comprehensive full-wave analysis of the optimized antenna using coaxial feed. Section H: Demonstrates the antenna's validation using an equivalent circuit model (ECM). Section I presents proposed antenna hardware and measurement validation. Finally, a summary of the proposed work is found in Section III, encapsulating the key findings and contributions of the novel antenna design.

## II. ANTENNA GEOMETRY AND WORKING MECHANISM

### A. Overall Antenna Design.

Fig. 1 shows the proposed tri-band antenna designed on FR4 dielectric material with  $\epsilon_r=4.3$  and a loss tangent of 0.025. The antenna is designed by incorporating three equilateral triangle slots in an elliptically shaped patch. The resonance frequency of the antenna can be controlled using three parameters  $R_1$ ,  $R_2$ , and  $d$ . The electromagnetic power is supplied through a  $50\Omega$  coaxial feed probe from the bottom to the patch. The design and simulation were carried out using the electromagnetic simulation tool CST Studio Suite. The proposed antenna has a simple structure, making it easy for fabrication and integration into a circuit. The Table I shows the designed parameters of proposed antenna.

TABLE I  
PROPOSED ANTENNA PARAMETERS

Parameter	Value(m)	Parameter	Value(m)
L	40	R1	14
h	1.6	R2	8
d	8	t	0.035
$x_f$	0.8	$y_f$	2.1

### B. Cavity Model Method Discussion.

The cavity model is commonly applied to study the characteristics of microstrip antennas, providing valuable insights into their resonance modes and overall performance. In this model, the antenna's

radiating patch is treated as a resonant cavity with specific boundary conditions that simplify the analysis of its electromagnetic fields and resonant frequencies. The top surface of the cavity, represented by the metallic patch, and the bottom surface, represented by the ground plane, are assumed to be perfect electric conductors (PECs). This condition implies that the tangential component of the electric field is zero at these surfaces. Conversely, the side walls of the cavity, which correspond to the edges of the patch, are modeled as perfect magnetic conductors (PMCs). This boundary condition enforces that the tangential magnetic field component is zero along the edges. In microstrip antennas, the cavity model includes not only the patch and the ground plane but also accounts for the substrate and other elements within the structure, as illustrated in Fig. 2. For circular patch antennas, a key design parameter—the radius of the patch ("R")—controls the order of resonance modes. The  $TM_{mno}^z$  modes resonance frequency of circular patch is given below [20].

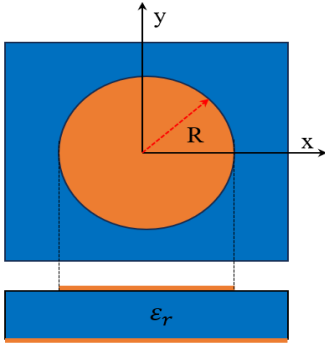


Fig.2. Circular patch antenna.

$$(f_r)_{mno} = \frac{1}{2\pi\sqrt{\mu\epsilon}} \left( \frac{\chi'_{mn}}{R} \right) \quad (1)$$

Where,  $\chi'_{mn}$  denotes the roots of the derivative of the Bessel function, these roots determine the orders of resonant frequencies, For the first order or dominant mode, the specific value is 1.8412, and corresponding  $TM_{110}^z$  (dominant mode) frequency is given by [20]

$$(f_r)_{110} = \frac{1.8412}{2\pi R\sqrt{\mu\epsilon}} = \frac{1.8412\theta_0}{2\pi R\sqrt{\epsilon_r}} \quad (2)$$

The design parameter 'R=17.67mm,' corresponding to the 2400 MHz (dominant mode) for a circular patch antenna on an FR/4 substrate with a dielectric constant of 4.3 and a loss tangent of 0.025, has been identified using equation (2).

While the cavity model provides valuable insights, it has limitations. It may not accurately represent the behavior of irregularly shaped antennas or those with complex structures. The characteristic mode analysis method represented in next section, which is design and optimized irregularly shaped or complex structure antenna.

### C. Parameters and topological optimization using CMA.

Characteristic Mode Theory (CMT) is a theoretical framework used in antenna engineering to analyze and design antennas based on their characteristic modes. CMT helps in understanding these modes and their influence on antenna performance. This methodology serves as a systematic design approach, aiming to offer a comprehensive physical understanding of conducting structures. This sets it apart from alternative methods like automated optimization or trial-and-error, which lack the capacity to reveal the physical behavior of circuits[16,21-22].

These current modes represent intrinsic characteristics of the conducting electromagnetic body and are derived by solving the Eigenvalue equation, as detailed in references [21-24].

#### 1. Resonance Condition:

1. At resonance, the corresponding eigenvalue is zero ( $e_n = 0$ ), indicating a special condition where the system is in a resonant state [16,21,23].

#### 2. Energy Storage:

1. Positive Eigenvalues ( $e_n > 0$ ) signify the storing of magnetic energy.
2. Negative Eigenvalues ( $e_n < 0$ ) indicate the storing of electric energy [21,28].

#### 3. Modal Significance for $n$ mode

$$MS = \frac{1}{|1+je_n|} \quad (1)$$

The intrinsic property of each mode, known as modal significance (MS), remains unaffected by external stimulus sources [16,23-24]. In quantitative terms, MS relies solely on the eigenvalues, where a smaller  $e_n$  corresponds to a higher radiation efficiency for the associated characteristic current,  $J_n$ . As  $e_n$  approaches zero, the characteristic current  $J_n$  demonstrates resonant radiation. The modal significance effectively transforms the eigenvalue range from  $+\infty$  to  $-\infty$  into a more constrained range of 0 to 1 [16,30-].

#### 4. Characteristics Angle (CA)

$$CA = 180^\circ - \tan^{-1}(e_n) \quad (2)$$

The characteristic angle,  $CA = 180$ , directly represents the phase difference between the related characteristic field and the characteristic current; this indicates that the  $n$ th mode is in resonance [16, 23–26].

#### D. CMA Analysis of Antenna-1.

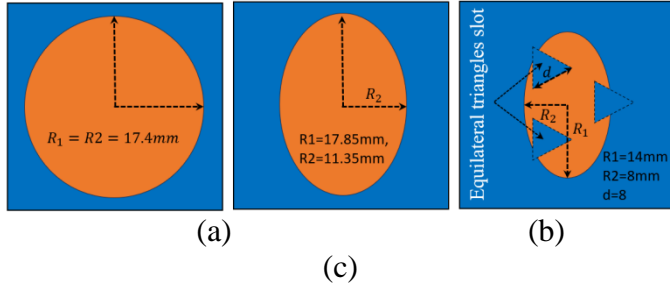


Fig.3. shows multi band antenna design steps: (a) antenna-1, (b) antenna-2 and, (c) antenna-3.

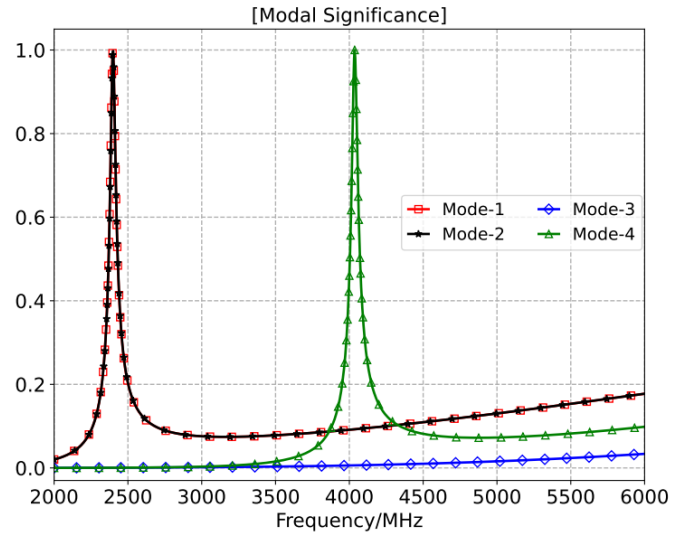


Fig. 4. Modal significant plots for Antenna-1

The initially circular patch antenna is designed using the initial design parameter  $R=17.4$  mm at 2400 MHz from the cavity model method, as shown in Fig.3(a). The circular antenna is analyzed up to the fourth mode, and its modal significance plots are represented in Fig.4. The maximum values of the modal significance plot represent the resonance behavior of the conducting body, contributing to maximum radiation for associated characteristic modes. At the same frequency of 2400 MHz, mode-1 and mode-2 have significance for radiation (because of  $MS_n > 1/\sqrt{2}$ ). Similar to this, mode-4 at 4036 MHz has significance for radiation (since  $MS_n > 1/\sqrt{2}$ ) [24].

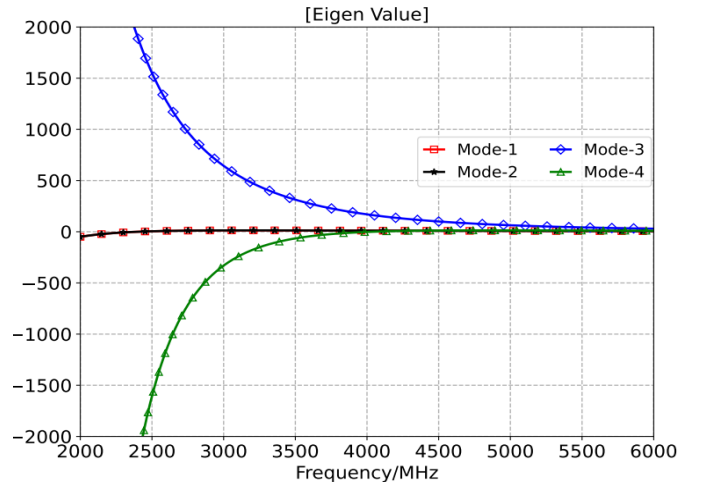


Fig. 5. Eigen value plots for Antenna-1

However, in the case of radiation, mode-3 is not significant (because  $MS_n = 0$ ). Fig. 5 shows the eigen plot for antenna-1. In the plot, mode-1 and mode-2 exhibit  $e_n = 0$ , indicating resonance for radiation. At this state, electric and magnetic energy are balanced. Mode-3 has an eigenvalue  $e_n > 0$ , signifying stored magnetic energy not associated with radiation. Mode-4, at lower frequencies, stores electric energy due to  $e_n < 0$ . However, at 4036 MHz, it achieves a balance between electric and magnetic energy due to  $e_n = 0$ , making it significant for radiation.

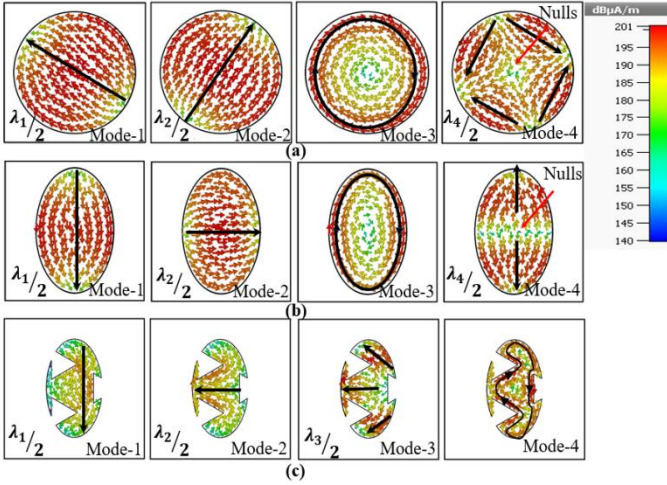


Fig.6. Surface current distribution on antennas: (a) Antenna-1, (b) Antenna-2, and (c) Antenna-3

The Fig. 6(a) illustrates the surface current distribution behavior of the conducting body for the associated characteristic modes. The surface current arrows depict the orthogonality behavior between mode-1 and mode-2, showcasing a pure  $\lambda_1/2$  current distribution. This indicates that they exhibit a dominant mode of antenna behavior. Furthermore, the mode-3 shows a closed-loop formed surface current distribution in the antenna, indicating a magnetic mode and not significant for radiation. In contrast, the mode-4 is significant for radiation, and its surface current distribution reveals four  $\lambda_4/2$  current distributions, indicating a higher order mode with surface currents nulls at center. The radiation performance of antenna can be analysis form associated characteristic modes. Fig.7(a) displays the antenna-1 radiation pattern in up to four modes. There is a broadside radiation pattern in modes 1 and 2, mode-3 have conical shaped radiation pattern, and mode-4 also have conical shaped pattern due to

surface current nulls at center of antenna. This higher order mode (mode-4) needs to improvement in broadside pattern for multi band antenna characteristics.

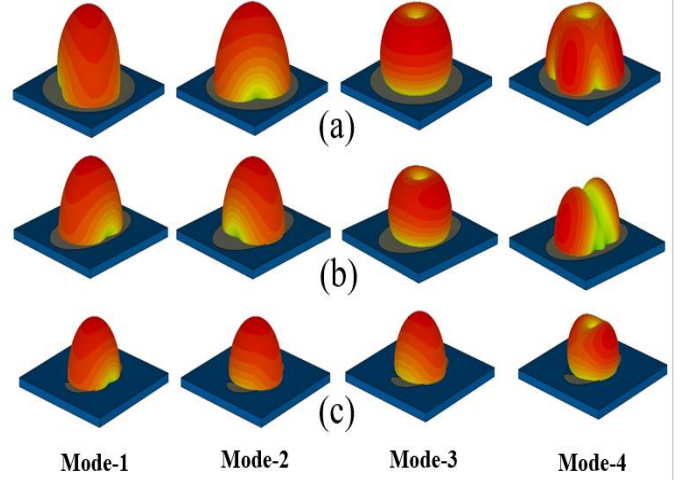


Fig.7. Shows the radiation patterns for, (a) Antenna-1, (b) Antenna-2, and (c) Antenna-3

#### E. CMA Analysis of Antenna-2

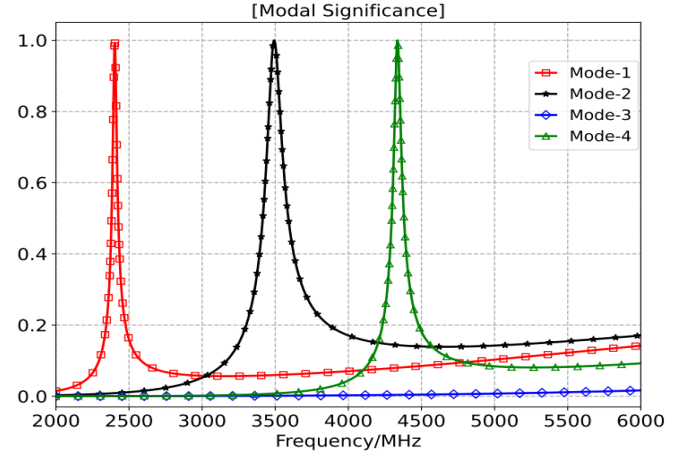


Fig. 8. Modal significant plots for Antenna-2.

To get tri band characteristics in antenna, we need further modified antenna-1, because antenna-1 only has 2400 MHz desire band for Wi-Fi . With an improved higher-order mode radiation pattern, surface current modification in an antenna may be used to modify the remaining two bands, 3500MHz for 5G and 5200MHz for Wi-Max. The antenna is optimized using CMA and adjusted the resonance mode-1 at 2400MHz and mode-2 at 3500MHz with design parameters  $R_1=17.85\text{mm}$ , and  $R_2=11.35\text{mm}$  as shown in Fig3(b) and its corresponding modal

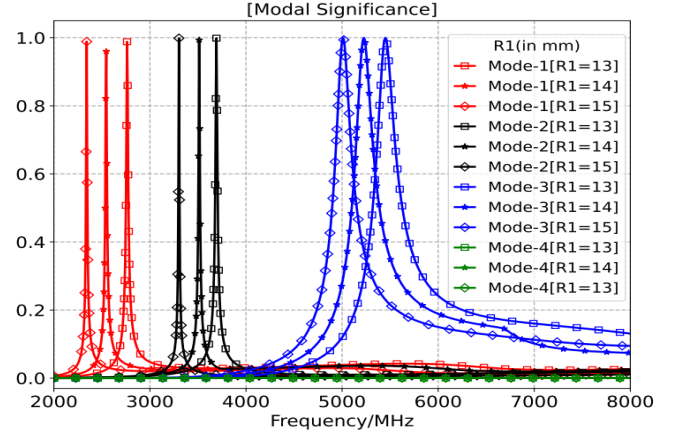
significant plots shown in Fig.8. While modes 1 through 4 have significance for radiation, mode 3, which is a magnetic mode, is not significant for radiation. The antenna-2 surface current distribution is seen in Fig.6. The surface current arrows of mode-1 and mode-2 showcase a pure  $\lambda_1/2$  current distribution, indicating a dominant mode of antenna behavior. This suggests that these modes exhibit a primary role in the antenna's overall performance.

Additionally, mode-3 displays a closed-loop formed surface current distribution, signifying a magnetic mode that is not significant for radiation. In contrast, mode-4 is found to be significant for radiation. Its surface current distribution reveals  $\lambda_4/2$  current distributions, indicating a higher order mode with surface current nulls at the center. Mode-1 and mode-2 exhibit the desired frequencies at 2400 MHz and 3500 MHz, respectively, along with broadside radiation patterns. However, mode-4 has not shown improvement in broadside radiation, as evidenced by its surface current nulls at the center of the antenna, as depicted in Fig. 7. Despite efforts to optimize the antenna for tri-band operation, the radiation characteristics of mode-4 have not been enhanced in terms of broadside radiation. Further adjustments may be needed to address this limitation and improve the overall performance of mode-4 in achieving the desired radiation patterns.

#### F. CMA Analysis of Antenna-3

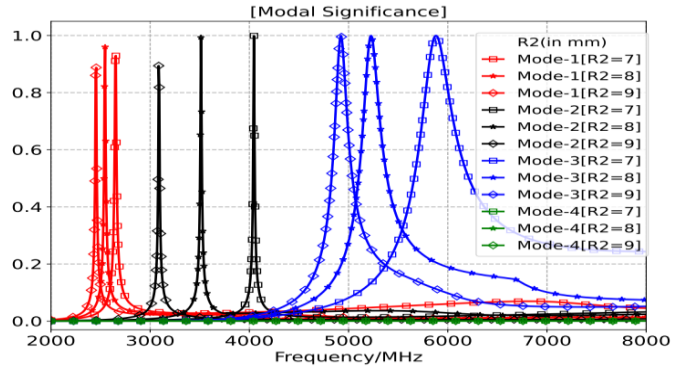
The dual-band characteristics of antenna-2 are achieved with resonance frequencies at 2400 MHz and 3500 MHz for Wi-Fi and 5G Sub-6 band, respectively, exhibiting broadside radiation patterns. The modified antenna, shown in Fig. 3(c), incorporates design parameters  $R1=17.85\text{mm}$ ,  $R2=11.35\text{mm}$ , and  $d=4\text{mm}$ . To achieve a broadside pattern in a higher-order mode with a shifted resonance frequency at 5200 MHz, the antenna is slotted with equilateral triangles. The corresponding modal significance plots for antenna-3 are shown in Fig. 9. Since  $MS_n > 1/\sqrt{2}$ , mode-1, mode-2, and mode-3 in this figure are significant for radiation, however mode-4 is linked to non-significance for radiation. Fig.6 illustrates the surface current distribution of antenna-3, where mode-1 and mode-2 display orthogonal surface current polarities for pure  $\lambda_1/2$  and pure  $\lambda_2/2$ , respectively. However, mode-3 exhibits three components of surface current  $\lambda_3/2$  in the same direction, indicating no nulls in the antenna

center. Consequently, all surface current components add constructively, resulting in broadside radiation patterns, as represented in Fig. 7.

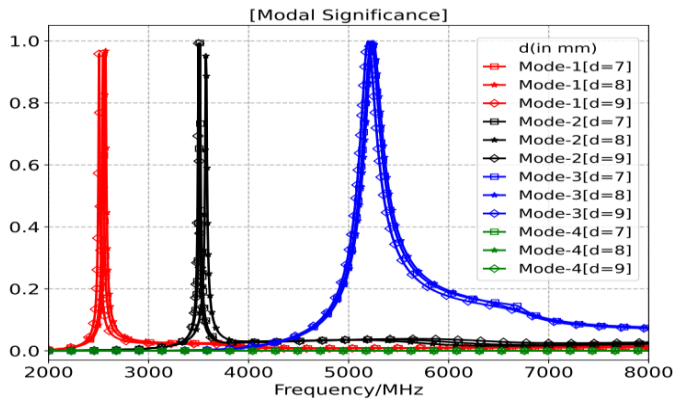


(a)

Therefore, mode-1, mode-2, and mode-3 collectively contribute to achieving tri-band characteristics with broadside radiation patterns at 2400 MHz, 3500 MHz, and 5200 MHz for Wi-Fi, 5G Sub-6, and Wi-Max, respectively.



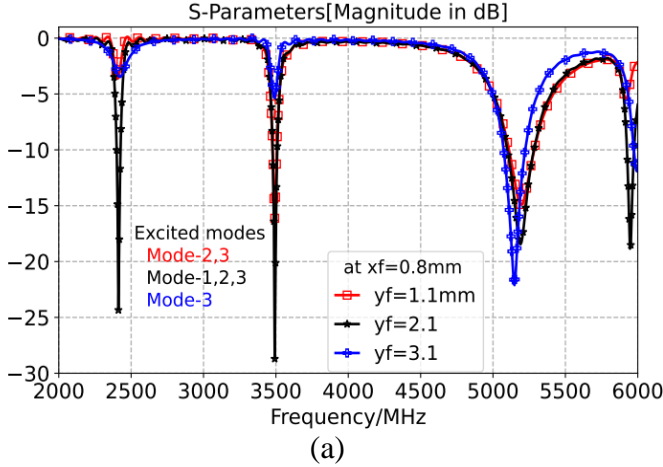
(b)



(c)

Fig. 9. Modal significant plots for Antenna-3 parametric study: (a) Parameter “R1”, (b) Parameter “R2”, Parameter “d”.

### G. Full Wave EM analysis of Proposed antenna



After Characteristics Mode Analysis (CMA), the desired modes (mode-1, mode-2, and mode-3) for WiFi, 5G Sub-6, and Wi-Max are excited using a coaxial feed in a full-wave simulation. The coaxial feed location has been fine-tuned through a parametric study, resulting in optimized coordinates of  $x_f=0.8$  mm and  $y_f=2.1$  mm. The resonant characteristics are illustrated in the scattering (S11) parameter plot in Fig.10 (a, b).

The operating resonant bands are identified as 2400 MHz (Wi-Fi), 3500 MHz (5G Sub-6), and 5200 MHz (Wi-Max) respectively. These resonant bands are depicted in the associated gain plot shown in Fig.11. Each band exhibits broadside radiation characteristics with gains of 5.59 dBi, 6.19 dBi, and 6.8 dBi at 2400 MHz, 3500 MHz, and 5200 MHz, respectively. The optimized coaxial feed location and resonant characteristics ensure enhanced performance across the specified frequency bands, making the antenna well-suited for applications in WiFi, 5G Sub-6, and Wi-Max communication systems.

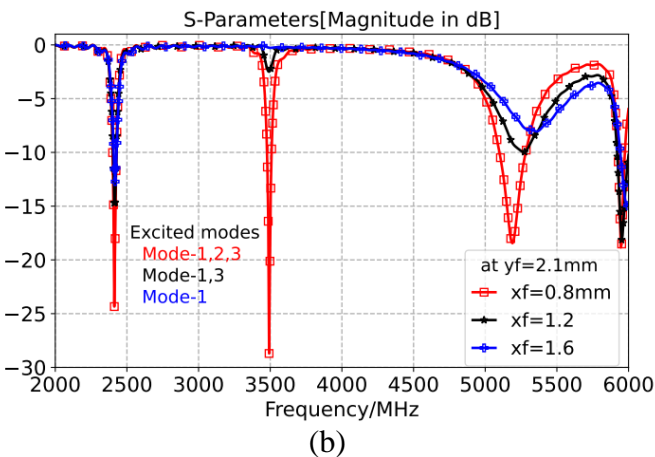


Fig.10. S11 plots of proposed antenna with different values of  $x_f$  and  $y_f$ . (a) For  $x_f(y_f=2.1$  mm), (b) for  $y_f(x_f=0.8$ mm).

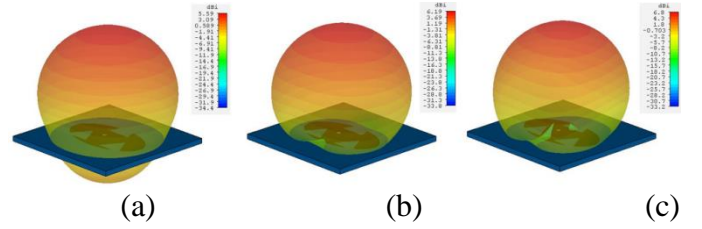


Fig.11. shows the gain of proposed antenna (a)  $f=2400$  MHz, (b)  $f=3500$  MHz, and (c)  $f=5200$  MHz.

### H. Equivalent circuit modeling (ECM) of Proposed antenna

The proposed antenna is electrically validated through equivalent circuit modeling using RLC parameters, as illustrated in Fig. 12. The significant modes, i.e., mode-1 (2400MHz), mode-2 (3500MHz), and mode-3 (5200MHz), are represented by electrical parameters  $R_1L_1C_1$ ,  $R_2L_2C_2$ , and  $R_3L_3C_3$ , respectively, with the coaxial feed line represented by  $L_fC_f$ . The proposed equivalent circuit model (ECM) is simulated using the CST circuit simulation tool, and the electrical parameters are optimized accordingly for mode-1, mode-2, and mode-3 resonance frequencies. Fig. 13 illustrates a comparison of S11 plots between the ECM circuit and 3D electromagnetic simulation results. The optimized parameters are represented in Table II.

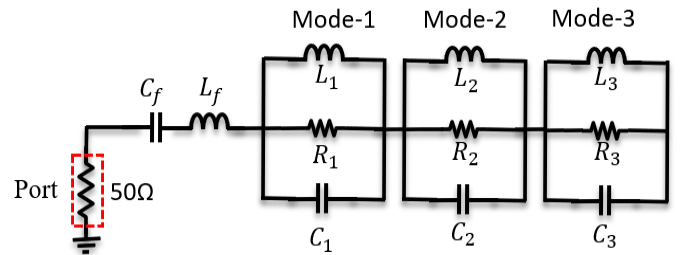


Fig.12. Equivalent circuit of proposed antenna.

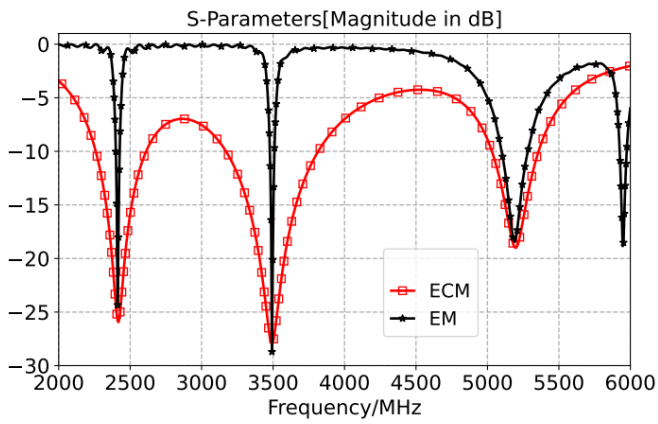


Fig.13. Comparison of S11 plot between Electromagnetic simulation and equivalent circuit model simulation.

TABLE II  
ELECTRICAL PARAMETERS OF ECM

$C_f$ (pF)	$L_f$ (nH)	$R_1$ (ohm)	$L_2$ (nH)	$C_2$ (pF)	$R_2$ (ohm)
7.37	0.34	44	0.11	8.38	37.82
$L_1$ (nH)	$C_1$ (pF)		$R_3$ (ohm)	$L_3$ (nH)	$C_3$ (pF)
0.54	8.24		51.81	0.50	4.05

### 1. Proposed Antenna Hardware Verification.



(a)



(b)

Fig.14. shows the fabricated prototype of the proposed antenna: (a) front view and (b) bottom view.

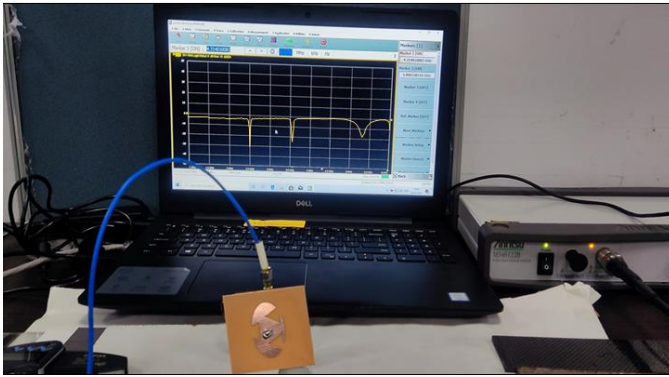


Fig.15. S11 measurement arrangement using VNA.

A copper-clad FR-4 epoxy substrate ( $\epsilon_r=4.3$ ,  $\tan\delta = 0.02$ ), is used to execute the antenna design. The front and bottom views of the printed antenna are shown in Fig. 14. The proposed antenna design has been verified using a Vector Network Analyzer (VNA) to ensure its validity. Fig. 15 shows the setup for using the VNA to measure S11 parameters. A comparison of the S11 plots between the measured and simulated results is shown in Fig. 16, which shows a good agreement.

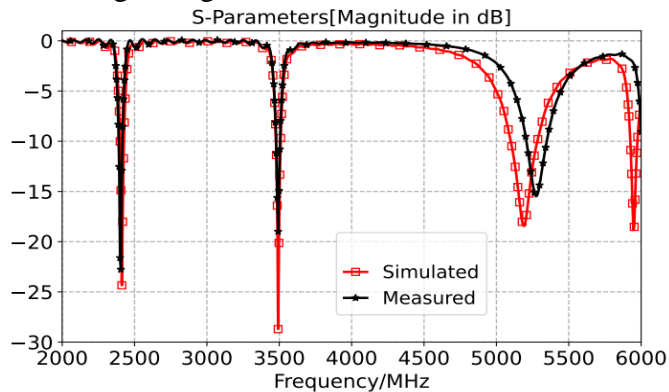


Fig.16. S11 plots from simulation and measurement.

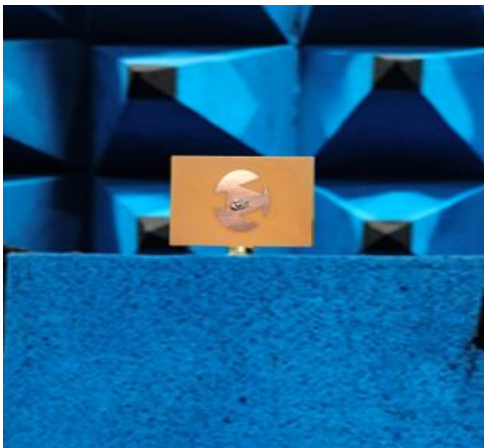


Fig.17. Presents the far field pattern measurement in an anechoic chamber.

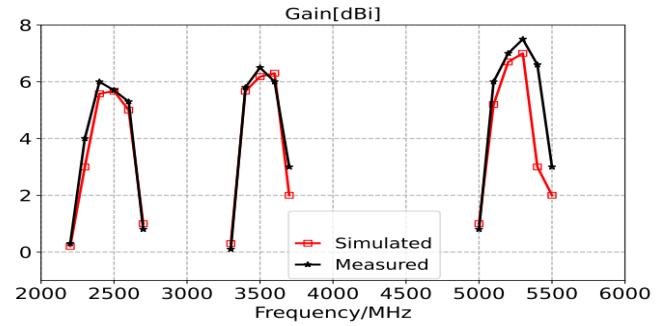
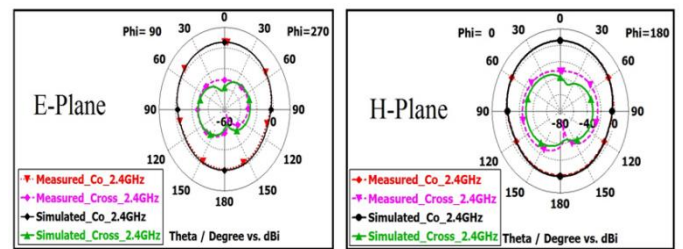
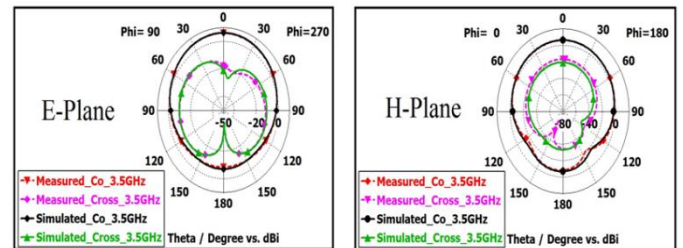


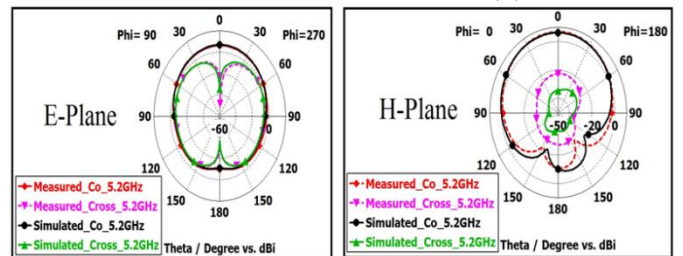
Fig.18. Simulated and Measured Gain of proposed antenna.



(a)



(b)



(c)

Fig.19. Far field simulate and measured performance of antenna:(a) at 2400MHz, (b) at 3500 MHz, and (c) at 5200MHz.

Figure 17 shows the far-field pattern measurement setup inside an anechoic chamber, where the antenna was tested in a reflection-free environment to accurately capture its radiation characteristics. Figure 18 presents a comparison of simulated and measured gain across three operating frequency

bands, showing good alignment between simulated and measured results, with minor variations attributed to fabrication and measurement tolerances. Figure 19 further evaluates the antenna's directional performance by illustrating the simulated and measured far-field radiation patterns in both the E-plane and H-plane at 2400 MHz, 3500 MHz, and 5200 MHz. The close match between simulated and measured co-polarized and cross-polarized components across these figures validates the antenna's multiband functionality, gain, and directional stability.

TABLE III  
RELATIVE WORK COMPARISON TABLE  
WITH PROPOSED ANTENNA

Ref.	Size ( $\lambda_o$ )	Frequency Bands (GHz)	Impedance Bandwidth (%)	Gain (dBi)	Broadside Radiation Patterns
1	0.29 $\times 0.29$	3.06, 4.84, 7.5	25.81, 19.62, 8.40	2.75, 5.95, 3.45	no
12	0.29 $\times 0.47$	3.56, 4.83, 5.84	1.36, 2.48, 1.69	5.01, 6.89, 5.83	no
18	0.3 $\times 0.3$	1.8, 5.8, 10	22.5, 21.55, 4.8	2.1, 4.2, 3.8	no
19	0.32 $\times 0.32$	2.45, 5.8, 14	31.42, 20.55, 43.07	2.41, 4.46, 5	no
27	0.13 $\times 0.21$	2.45, 3.5, 5.8	22.04, 15.14, 25.86	-0.5, 1.2, 3.1	yes
<b>This work</b>	<b>0.32 <math>\times 0.32</math> 2</b>	<b>2.4, 3.5, 5.2</b>	<b>1.08, 1, 2.88</b>	<b>6, 6.5, 7.5</b>	<b>yes</b>

Table-III provides a comprehensive performance comparison between our proposed antenna and various multi-band antennas from prior studies. Our antenna distinguishes itself with a low-profile and straightforward design approach, exhibiting broadside radiation patterns across all bands. This makes it a compelling choice for a wide range of

wireless communication applications, delivering enhanced performance.

### III. CONCLUSION

A tri-band antenna with a single coaxial feed, featuring desirable characteristics for Wi-Fi, 5G Sub-6, and Wi-Max, is demonstrated in this study. The tri-band functionality is achieved by modifying a circular patch antenna into an elliptical shape loaded with three equilateral triangle slots, employing the characteristics mode analysis method. The surface currents are reshaped by strategically loading the equilateral triangle slots to eliminate surface current nulls at the center of the patch, thereby improving the radiation pattern in the broadside direction. The optimized modes in the proposed antenna are excited using full-wave electromagnetic simulation. Additionally, the antenna's performance is validated through an equivalent circuit model and hardware testing. The CST Studio Suite is utilized for both the design and simulation of the antenna, which operates at frequencies of 2406 MHz, 3491 MHz, and 5274 MHz, respectively.

### REFERENCES

- [1] Chetouah, Farouk, Nacerdine Bouzit, Idris Messaoudene, Salih Aidel, Massinissa Belazzoug, and Youcef Braham Chaouche. "Annular dielectric resonator loaded with strip loop antenna for tri-band applications." In 2017 13th International Wireless Communications and Mobile Computing Conference (IWCMC), pp. 861-865. IEEE, 2017.
- [2] Yan, Binyun, Weixing Sheng, Jie Cui, and Jie Lu. "Compact wideband CPW-fed tri-band antenna with multi-shaped strips for WLAN/WiMAX applications." In 2019 49th European Microwave Conference (EuMC), pp. 240-243. IEEE, 2019.
- [3] Cao, Y. F., S. W. Cheung, and T. I. Yuk. "A multiband slot antenna for GPS/WiMAX/WLAN systems." IEEE Transactions on Antennas and Propagation 63, no. 3 (2015): 952-958.
- [4] Yahia, Benghanem, Mansoul Ali, and Mouffok Lila. "Compact Tri-Band Two-

- Element MIMO Slot Antenna for 5G Sub-6 GHz Frequency Bands." In 2022 2nd International Conference on Advanced Electrical Engineering (ICAEE), pp. 1-6. IEEE, 2022.
- [5] Sathishkumar, N., V. Nandalal, and Rajesh Natarajan. "Design of a Compact Double-Square-Ring-Shaped Dual-Band Antenna for WiMAX/WLAN Applications." *Wireless Personal Communications* 128, no. 3 (2023): 2073-2084.
- [6] Jarchavi, Syed Muhammad Rizvi, Mohsin Iqbal, Mariana Dalarsson, Mohammad Alibakhshikenari, and Iyad Dayoub. "Compact Multi-Band Flexible Antenna for ISM, WLAN, Wi-Fi, and 5G sub-6-GHz Applications." In 2022 3rd URSI Atlantic and Asia Pacific Radio Science Meeting (AT-AP-RASC), pp. 1-3. IEEE, 2022.
- [7] Kamran, Areeba, Fareah Tariq, Qudsia Amjad, Rashid Karim, and Arshad Hassan. "A bus shaped tri-band antenna for Sub-6 GHz 5G wireless communication on flexible PET substrate." In 2019 22nd International Multitopic Conference (INMIC), pp. 1-6. IEEE, 2019.
- [8] Feng, Botao, Baifa Yang, Li Deng, Zhengdong Zhou, and Xiao Ding. "A Compact Vehicle-Mounted Garden-Themed Artistic Antenna With Isolation Improvement for 2 G/3 G/LTE/5 G Sub-6-GHz/WiFi/Bluetooth Communications." *IEEE Transactions on Vehicular Technology* (2022).
- [9] Alam, Md Mottahir, Rezaul Azim, Nebras M. Sobahi, Asif Irshad Khan, and Mohammad Tariqul Islam. "A dual-band CPW-fed miniature planar antenna for S-, C-, WiMAX, WLAN, UWB, and X-band applications." *Scientific Reports* 12, no. 1 (2022): 7584.
- [10] Ullah, Shakir, Inzamam Ahmad, Yasir Raheem, Sadiq Ullah, Toufeeq Ahmad, and Usman Habib. "Hexagonal shaped CPW feed based frequency reconfigurable antenna for WLAN and sub-6 GHz 5G applications." In 2020 International Conference on Emerging Trends in Smart Technologies (ICETST), pp. 1-4. IEEE, 2020.
- [11] Dildar, Haris, Faisal Althobiani, Ikhlas Ahmad, Wasi Ur Rehman Khan, Sadiq Ullah, Naveed Mufti, Shakir Ullah, Fazal Muhammad, Muhammad Irfan, and Adam Glowacz. "Design and experimental analysis of multiband frequency reconfigurable antenna for 5G and sub-6 GHz wireless communication." *Micromachines* 12, no. 1 (2021): 32.
- [12] Kwame, Oteng Gyasi, Yongjun Huang, Guangjun Wen, Affum Emmanuel Ampoma, and Wei Hu. "Tri-band planar monopole antenna with dual band circular polarization." In 2017 IEEE International Symposium on Antennas and Propagation & USNC/URSI National Radio Science Meeting, pp. 2533-2534. IEEE, 2017.
- [13] Jha, Kumud Ranjan, Nishu Rana, and Satish Kumar Sharma. "Design of Compact Antenna Array for MIMO Implementation Using Characteristic Mode Analysis for 5G NR and Wi-Fi 6 Applications." *IEEE Open Journal of Antennas and Propagation* 4 (2023): 262-277.
- [14] Mudda, Shivleela, K. M. Gayathri, and Mudda Mallikarjun. "Wide-Band Frequency Tunable Antenna for 4G, 5G/Sub 6 GHz Portable Devices and MIMO Applications." *Prog. Electromagn. Res. C* 118 (2022): 25-41.
- [15] Sharma, Indra Bhooshan, Fateh Lal Lohar, Ravi Kumar Maddila, Abhinav Deshpande, and M. M. Sharma. "Tri-band microstrip patch antenna for C, X, and Ku band applications." In *Optical and Wireless Technologies: Proceedings of OWT 2017*, pp. 567-574. Springer Singapore, 2018.
- [16] Singh, Jaget, and Fateh Lal Lohar. "Frequency reconfigurable quad band patch antenna for radar and satellite applications using FR-4 material." *Materials Today: Proceedings* 28 (2020): 2026-2030.

- [17]Lohar, Fateh Lal, Chandresh Dhote, Yogesh Solunke, and Nitin Kumar Suyan. "Design of circularly polarized irnss receiver antenna using characteristic mode analysis." In 2019 IEEE Indian Conference on Antennas and Propagation (InCAP), pp. 1-5. IEEE, 2019.
- [18]Griffiths, Lance Allen, Cynthia Furse, and You Chung Chung. "Broadband and multiband antenna design using the genetic algorithm to create amorphous shapes using ellipses." IEEE Transactions on Antennas and Propagation 54, no. 10 (2006): 2776-2782.
- [19]Chaouche, Youcef Braham, Mourad Nedil, Boualem Hammache, and Massinissa Belazzoug. "Design of modified Sierpinski Gasket fractal antenna for tri-band applications." In 2019 IEEE International Symposium on Antennas and Propagation and USNC-URSI Radio Science Meeting, pp. 889-890. IEEE, 2019.
- [20]Wang, Zhong-Gen, Rui You, Ming Yang, Jinzhi Zhou, and Mingqing Wang. "Design of a Monopole Antenna for WiFi-UWB Based on Characteristic Mode Theory." *Progress in Electromagnetics Research M* 125 (2024).
- [21]Thanamalapong, Wutthipong, Chuwong Phongcharoenpanich, and Suthasinee Lamultree. "A tri-band antenna for 2.4/5 GHz WLAN and Ku-Band applications." In 2020 17th International Conference on Electrical Engineering/Electronics, Computer, Telecommunications and Information Technology (ECTI-CON), pp. 80-83. IEEE, 2020.
- [22]Balanis, Constantine A. *Antenna theory: analysis and design*. John Wiley & sons, 2016.
- [23]Li, Weiwen, Yongcong Liu, Jie Li, Longfang Ye, and Qing Huo Liu. "Modal proportion analysis in antenna characteristic mode theory." *International Journal of Antennas and Propagation* 2019 (2019).
- [24]Wang, Zhonggen, Mingqing Wang, and Wenyan Nie. "Design of a dual-band WiFi antenna using the theory of characteristic modes and nested Chinese characters." *Electronics* 12, no. 16 (2023): 3465.
- [25]Adams, Jacob J., Simone Genovesi, Binbin Yang, and Eva Antonino-Daviu. "Antenna element design using characteristic mode analysis: Insights and research directions." *IEEE Antennas and Propagation Magazine* 64, no. 2 (2022): 32-40.
- [26]Singh, Jaget, Fateh Lal Lohar, and B. S. Sohi. "Design of circular polarized patch antenna for NaviC receiver applications." In *IOP Conference Series: Materials Science and Engineering*, vol. 1033, no. 1, p. 012039. IOP Publishing, 2021.
- [27]Suo, Meng, Han Xiong, Xin-Ke Li, Qi-Feng Liu, and Huai-Qing Zhang. "A flexible transparent absorber bandwidth expansion design based on characteristic modes." *Results in Physics* 46 (2023): 106265.
- [28]Hu, Wei, Zhan Chen, Long Qian, Lehu Wen, Qi Luo, Rui Xu, Wen Jiang, and Steven Gao. "Wideband back-cover antenna design using dual characteristic modes with high isolation for 5G MIMO smartphone." *IEEE Transactions on Antennas and Propagation* 70, no. 7 (2022): 5254-5265.
- [29]Kollipara, Vamshi, and Samineni Peddakrishna. "Circularly polarized antennas using characteristic mode analysis: A review." *Advances in Technology Innovation* 7, no. 4 (2022): 242.
- [30]Wei, Yuming, Yuanxin Li, Zhixi Liang, Shao Yong Zheng, and Yunliang Long. "A tri-band patch antenna with dual rampart line structure." *IEEE Antennas and Wireless Propagation Letters* 21, no. 4 (2022): 793-797.
- [31]Sharma, Usha, Garima Srivastava, Mukesh K. Khandelwal, and Rashmi

- Roges. "Design Challenges and Solutions of Multiband MIMO Antenna for 5G/6G Wireless Applications: A Comprehensive Review." *Progress in Electromagnetics Research B* 104 (2024).
- [32]Yacoub, Ahmad, and Daniel N. Aloi. "Innovative Loaded Low-Profile Tri-Band MIMO Antenna System for Wi-Fi 7 Technology." *Progress in Electromagnetics Research M* 122 (2023).
- [33]Hussain, Musa, Wahaj Abbas Awan, Mohammed S. Alzaidi, and Dalia H. Elkamchouchi. "Self-decoupled tri band MIMO antenna operating over ISM, WLAN and C-band for 5G applications." *Helikon* 9, no. 7 (2023).
- [34]Gençoğlan, Duygu Nazan, Şule Çolak, and Merih Palandöken. "Spiral-resonator-based frequency reconfigurable antenna design for sub-6 ghz applications." *Applied Sciences* 13, no. 15 (2023): 8719.
- [35]Sehgal, Puneet, and Kamlesh Patel. "Triband dual port h-SRR MIMO antenna for WLAN/WiMAX/Wi-Fi 6 applications." *Progress In Electromagnetics Research M* 123 (2024): 35-43.
- [36]Pandya, Killol, Trushit Upadhyaya, Upesh Patel, Vishal Sorathiya, Aneri Pandya, Ahmed Jamal Abdullah Al-Gburi, and Mohd Muzafar Ismail. "Performance Analysis of Quad-Port UWB MIMO Antenna System for Sub-6 GHz 5G, WLAN and X Band Communications." *Results in Engineering* (2024): 102318.
- [37]Ellis, M. S., J. Nourinia, Ch Ghobadi, K. Hosseini, F. Alizadeh, and B. Mohammadi. "Compact wideband printed antenna with circularly polarized tilted beam radiation using a Quasi-Radiator." *AEU-International Journal of Electronics and Communications* 171 (2023): 154883.